

**DETC98/MECH-5947**

**IDENTIFICATION AND COMPENSATION OF GEOMETRIC AND ELASTIC ERRORS  
IN LARGE MANIPULATORS:  
APPLICATION TO A HIGH ACCURACY MEDICAL ROBOT**

Marco A. Meggiolaro  
Massachusetts Institute of Technology  
Department of Mechanical Engineering  
77 Massachusetts Ave, Cambridge, MA 02139  
USA, Tel 617-253-5095, Fax 617-258-7881

Constantinos Mavroidis  
Rutgers University  
Dept. of Mechanical and Aerospace Engineering  
98 Brett Road, Piscataway, NJ 08854  
USA, Tel 732-445-0732, Fax 732-445-3124

Steven Dubowsky  
Massachusetts Institute of Technology  
Department of Mechanical Engineering  
77 Massachusetts Ave, Cambridge, MA 02139  
USA, Tel 617-253-2144, Fax 617-258-7881

**ABSTRACT**

A method is presented to identify the source of end-effector positioning errors in large manipulators using experimentally measured data. Both errors due to manufacturing tolerances and other geometric errors and elastic structural deformations are identified. These error sources are used to predict, and compensate for, the end-point errors as a function of configuration and measured forces. The method is applied to a new large high accuracy medical robot. Experimental results show that the method is able to effectively correct for the errors in the system.

**INTRODUCTION**

Large robot manipulators are needed in field, service and medical applications to perform high accuracy tasks. Examples are manipulators that perform decontamination tasks in nuclear sites, space manipulators such as the Special Purpose Dexterous Manipulator (SPDM) and manipulators for medical treatment (Hamel et al., 1997; Vaillancourt and Gosselin, 1994; Flanz, 1996). In these applications, a large robotic system may need to have very fine precision. Its accuracy specifications may be very small fractions of its size. Achieving such high accuracy is difficult because of the manipulator's size and its need to carry relatively heavy payloads. Further, many tasks, such as space applications, require systems to be light weight so that structural

deformation errors may become relatively large. For such systems geometric errors due to machining tolerances, and errors due to elastic deformation, create significant end-effector errors.

Due to task constraints it is often not possible to use direct end-effector sensing in a closed-loop control scheme to improve the system accuracy. Therefore, there is a need for model based error identification and compensation techniques. While classical calibration methods can achieve such compensation for some systems, they cannot correct the errors in large systems with significant elastic deformations, because they do not explicitly consider the effects of task forces and structural compliance. Here a method is developed that considers both deformation and more classical geometric errors in a unified manner.

This method is applied here to a new important medical application of large manipulator systems. The manipulator is used as a high accuracy robotic patient positioning system in a radiation therapy research facility now being constructed at the Massachusetts General Hospital (MGH), the Northeast Proton Therapy Center (NPTC) (Flanz et al., 1995; Flanz et al., 1996). The robotic patient positioning system (PPS) places a patient in a high energy proton beam delivered from a rotating gantry structure (see Figure 1). The PPS is a six degree of freedom manipulator that covers a large workspace of more than 4m in radius while carrying patients weighing as

much as 300 lbs. Patients are finally immobilized on the "couch" attached to the PPS end-effector.

The PPS, combined with the rotating gantry that carries the proton beam, enables the beam to enter the patient from any direction, while avoiding the gantry structure. Hence programmable flexibility offered by robotic technology is needed.

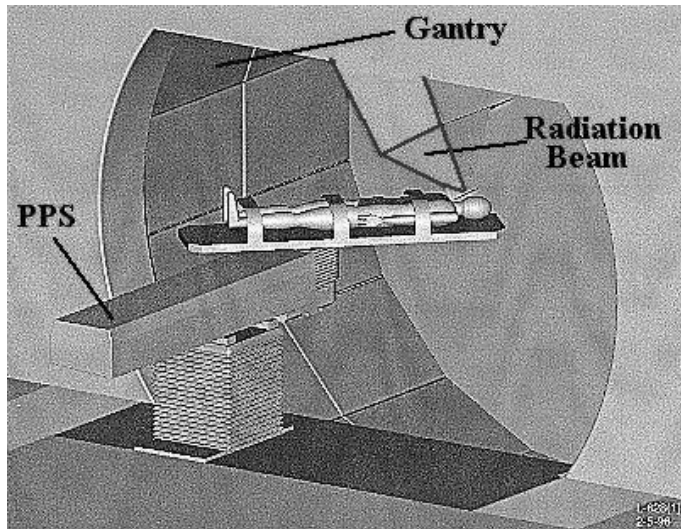


**Figure 1: Schematic of the PPS and the Gantry**

The required absolute positioning accuracy of the PPS is  $\pm 0.5$  mm. This accuracy is critical as larger errors may be dangerous to the patient (Rabinowitz et al., 1985). The required accuracy is roughly  $10^{-4}$  of the nominal dimension of system workspace. This is a greater relative accuracy than many industrial manipulators. In addition, FEM studies and experimental results show that the changing and heavy payload (between 1 and 300 pounds) creates end-effector errors due to elastic deformations of the order of 6-8 mm.

Considerable research has been performed in the model-based error compensation of manipulators, also called robot calibration (Roth, Mooring, Ravani, 1987; Hollerbach, 1988; Mooring, Roth and Driels, 1990; Zhuang and Roth, 1996; Hollerbach and Wampler, 1997). A major component of this process is the development of manipulator error models (Wu, 1984; Mirman and Gupta, 1993), some of them considering the effects of manipulator joint errors, while others focusing on the effects of link dimensional errors (Waldron and Kumar, 1979; Vaichav and Magrab, 1987). Some error models have been developed specifically for use in the calibration of manipulators (Broderick and Cirpa, 1988; Zhuang, Roth and Hamano, 1992; Zhuang, Wang and Roth, 1993), while some researchers have studied methods to find the optimal configurations to reduce the manipulator errors by calibration (Zhuang, Wang and Roth, 1994; Zhuang, Wu and Huang, 1996; Borm and Menq, 1991). Several calibration techniques have been used to improve robot accuracy through software

rather than changing the mechanical structure (Roth, Mooring and Ravani, 1986), including open and closed-loop methods (Whitney, Lozinski and Rourke, 1986; Hayati, Tso and Roston, 1988; Everett and Lin, 1988) as well as screw-axis measurement methods (Hollerbach and Wampler, 1996) sometimes combined with local calibration (Everett and Lei, 1995). Solution methods for the identification of the manipulator's unknown parameters have been studied for these model-based calibration processes (Dubowsky, Maatuk and Pereira, 1975; Zhuang and Roth, 1993). Most calibration methods have been applied to industrial or laboratory robots, achieving good accuracy when geometric errors are dominant. However, the existing calibration methods do not explicitly compensate for elastic errors due to the wrench at the end-effector. A calibration method that considers the weight dependency of the errors was developed (Drouet, Mavroidis and Dubowsky, 1998), but it needs an elastic model of the system.

In this paper a method that compensates for the position and orientation errors caused by geometric and elastic errors in large manipulators is presented. The method explicitly considers the weight dependency of the errors. An error model, developed by Mavroidis et al. (1997) and a set of experimentally measured positions and orientations of the robot end-effector, and measurements of the payload wrench, are used to calculate the robot "generalized" errors without needing a manipulator elastic model. Here, generalized are called the errors that characterize the relative position and orientation of frames defined at the manipulator links. They are found from measured data as a function of the configuration of the system and the task forces. Knowing these generalized errors the manipulator end-effector position and orientation errors are calculated and used at any configuration to correct the robot configuration to compensate for these errors. The method treats all errors of the manipulator such as geometric and elastic errors in a unified manner. The method is applied to Patient Positioning System. A force/torque sensor has been added to the system to measure the wrench applied by the patient's weight. It is experimentally shown to be able to reduce the inherent 5-7mm to less than the required accuracy of 0.5 mm.

## MODEL BASED ERROR COMPENSATION

There are many possible sources of errors in a manipulator. These errors are referred to as "physical errors", to distinguish them from "generalized errors" which are defined later. The main sources of physical errors in a manipulator are:

- **Mechanical system errors:** These errors are resulting from machining and assembly tolerances of the various manipulator mechanical components.

- **Deflections:** Elastic deformations of the members of the manipulator under load can result in large end-effector errors, especially in long reach manipulator systems.
- **Measurement and Control:** Measurement, actuator, and control errors that occur in the control systems will create end-effector positioning errors. The resolution of encoders and stepper motors are examples of this type of error.
- **Joint errors:** These errors include bearing run-out in rotating joints, rail curvature in linear joints, and backlash in manipulator joints and actuator gear box.

In most cases, physical errors are relatively small. However, their effect at the end-effector can be large.

Further, errors can be distinguished into “repeatable” and “random” errors (Slocum, 1992). Repeatable errors are errors whose numerical value and sign are constant for a given manipulator configuration. An example of a repeatable error is an assembly error. Random errors are errors whose numerical value or sign changes unpredictably. At each manipulator configuration, the exact magnitude and direction of random errors cannot be uniquely determined, but only specified over a range of values. Random errors cannot be compensated using classical calibration techniques. An example of a random error is the error that occurs due to backlash of an actuator gear train. Classical kinematic calibration and correction can only deal with repeatable errors. It will be shown experimentally in Section 4 that these errors dominate in the performance of the PPS.

To describe the kinematics of a manipulator the definition of reference frames at the manipulator base, end-effector, and at each of the joints that are characterized by the Denavit and Hartenberg parameters are defined (Craig, 1989). The position and orientation of a reference frame  $F_i$  with respect to the previous reference frame  $F_{i-1}$  is defined with a 4x4 matrix  $A_i$  that has the general form:

$$A_i = \begin{pmatrix} \mathbf{R}_i & \mathbf{T}_i \\ 0 & 1 \end{pmatrix} \quad (1)$$

The  $\mathbf{R}_i$  term is a 3x3 orientation matrix composed of the direction cosines of frame  $F_i$  with respect to frame  $F_{i-1}$  and  $\mathbf{T}_i$  is a 3x1 vector of the coordinates of center  $O_i$  of frame  $F_i$  in  $F_{i-1}$ . The elements of matrices  $A_i$  depend on the geometric parameters of the manipulator and the manipulator joint variables  $\mathbf{q}$ .

Physical errors change the geometric properties of a manipulator. As a result, the frames defined at the manipulator joints are slightly displaced from their expected, ideal locations. The position and orientation of a frame  $F_T^r$  with respect to its ideal location  $F_i^i$  is represented by a 4x4

homogeneous matrix  $E_i$ . The rotation part of matrix  $E_i$  is the result of the product of three consecutive rotations  $e_{si}$ ,  $e_{ri}$ ,  $e_{pi}$  around the Y, Z and X axes respectively. (These are the Euler angles of  $F_T^r$  with respect to  $F_i^i$ ). The subscripts s, r, and p represent spin (yaw), roll, and pitch, respectively. The translational part of matrix  $E_i$  is composed of the 3 coordinates  $e_{xi}$ ,  $e_{yi}$  and  $e_{zi}$  of point  $O_T^r$  in  $F_i^i$ . The 6 parameters  $e_{xi}$ ,  $e_{yi}$ ,  $e_{zi}$ ,  $e_{si}$ ,  $e_{ri}$  and  $e_{pi}$  are called here "generalized error" parameters. For a  $n^{\text{th}}$  degree of freedom manipulator, there are 6n generalized errors which can be written in vector form as  $\boldsymbol{\varepsilon} = [\dots, e_{xi}, e_{yi}, e_{zi}, e_{si}, e_{ri}, e_{pi}, \dots]$ , with i ranging from 1 to n. Since the physical errors are small, the generalized errors  $e_{xi}$ ,  $e_{yi}$ ,  $e_{zi}$ ,  $e_{si}$ ,  $e_{ri}$  and  $e_{pi}$  are also small, so a first order approximation can be applied to their trigonometric functions and products. Matrix  $E_i$ , after the first order approximation, has the form:

$$E_i = \begin{pmatrix} 1 & -e_{ri} & e_{si} & e_{xi} \\ e_{ri} & 1 & -e_{pi} & e_{yi} \\ -e_{si} & e_{pi} & 1 & e_{zi} \\ 0 & 0 & 0 & 1 \end{pmatrix} \quad (2)$$

The generalized errors can be calculated from the physical errors link by link and they depend on the system geometry, the system weight if they contain elastic errors, and the system joint variables.

The end-effector position and orientation error  $\Delta\mathbf{X}$  is defined as the 6x1 vector that represents the difference between the real position and orientation of the end-effector and the ideal or desired one:

$$\Delta\mathbf{X} = \mathbf{X}_T^r - \mathbf{X}_T^i \quad (3)$$

where,  $\mathbf{X}_T^r$  and  $\mathbf{X}_T^i$  are the 6x1 vectors composed of the three positions and three orientations of the end-effector reference frame ( $F_n$ ) in the inertial reference system ( $F_0$ ) for the real and ideal case, respectively.

When the generalized errors are considered in the model, the manipulator loop closure equation takes the form:

$$A_T(\mathbf{q}, \boldsymbol{\varepsilon}, \mathbf{s}) = A_1 E_1 A_2 E_2 \dots A_n E_n \quad (4)$$

where  $A_T$  is a 4x4 homogeneous matrix of the type shown in Equation (1) that describes the position and orientation of the end-effector frame  $F_6$  with respect to the inertial reference frame  $F_0$  as a function of the configuration parameters  $\mathbf{q}$ , the vector of the generalized errors  $\boldsymbol{\varepsilon}$ , and the vector of the structural parameters  $\mathbf{s}$ . The three components of the vector  $\mathbf{T}_T$  and the three angles of the rotation matrix  $\mathbf{R}_T$  are the six coordinates of vector  $\mathbf{X}_T^r$  that can be written in a general form:

$$\mathbf{X}_T^r = \mathbf{f}^r(\mathbf{q}, \boldsymbol{\varepsilon}, \mathbf{s}) \quad (5)$$

where  $\mathbf{f}^r$  is a vector non-linear function of  $\mathbf{q}$ ,  $\boldsymbol{\varepsilon}$ , and  $\mathbf{s}$ .

Since the generalized errors are small,  $\Delta \mathbf{X}$  can be calculated by the following linear equation in  $\boldsymbol{\varepsilon}$ :

$$\Delta \mathbf{X} = \mathbf{J}_e \boldsymbol{\varepsilon} \quad (6)$$

where  $\mathbf{J}_e$  is the  $6 \times 6n$  Jacobian matrix of the function  $\mathbf{f}^r$  with respect to the elements of the generalized error vector  $\boldsymbol{\varepsilon}$ . The elements of  $\mathbf{J}_e$  are defined as:

$$\mathbf{J}_e [i, j] = \frac{\partial \mathbf{f}^r [i]}{\partial \boldsymbol{\varepsilon} [j]} \quad (7)$$

The value of  $i$  ranges from 1 to 6 and  $j$  ranges from 1 to  $6n$ . In general  $\mathbf{J}_e$  depends on the system configuration, geometry and weight if there are elastic deflections in the system. More information on the development of the error model can be found in Mavroidis et al. (1997).

If the generalized errors,  $\boldsymbol{\varepsilon}$ , are known then the end-effector position and orientation error can be calculated using Equation (6). Figure 2 shows how an error model of the type of Equation (6) can be used in an error compensation algorithm. The method to obtain  $\boldsymbol{\varepsilon}$  is explained in Section 3.

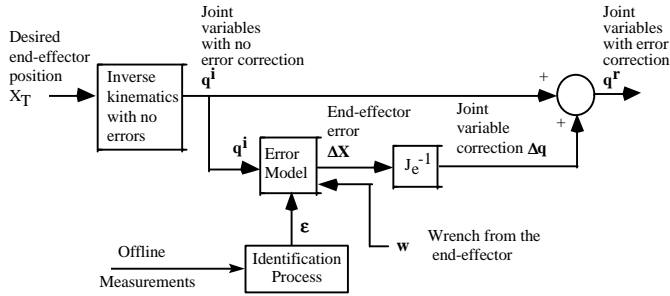


Figure 2: Error Compensation Scheme

## IDENTIFICATION OF THE GENERALIZED ERRORS

The first step in the method is to calculate the generalized errors,  $\boldsymbol{\varepsilon}$ , from off-line measurement data. The identification method to calculate  $\boldsymbol{\varepsilon}$  is based on the assumption that some components of vector  $\Delta \mathbf{X}$  can be obtained experimentally at a finite number of different manipulator configurations. However, since position coordinates are much easier to measure in practice than orientations, in many cases only the three position coordinates of  $\Delta \mathbf{X}$  are measured, requiring then twice the number of measurements for the calculation.

Assuming that all 6 components of  $\Delta \mathbf{X}$  can be measured, for an  $n^{\text{th}}$  degree of freedom manipulator, its  $6n$  generalized errors  $\boldsymbol{\varepsilon}$  can be calculated by fully measuring vector  $\Delta \mathbf{X}$  at  $n$  different configurations and then writing Equation (6)  $n$  times:

$$\Delta \mathbf{X}_T = \begin{bmatrix} \Delta \mathbf{X}_1 \\ \Delta \mathbf{X}_2 \\ \dots \\ \Delta \mathbf{X}_n \end{bmatrix} = \begin{bmatrix} \mathbf{J}_e(q_1, w_1) \\ \mathbf{J}_e(q_2, w_2) \\ \dots \\ \mathbf{J}_e(q_n, w_n) \end{bmatrix} \cdot \boldsymbol{\varepsilon} = \mathbf{J}_T \cdot \boldsymbol{\varepsilon} \quad (8)$$

where  $\Delta \mathbf{X}_T$  is the  $6n \times 1$  vector formed by all measured vectors  $\Delta \mathbf{X}$  at the  $n$  different configurations and  $\mathbf{J}_T$  is the  $6n \times 6n$  total Jacobian matrix formed by the  $n$  error Jacobian matrices at the  $n$  configurations.

If matrix  $\mathbf{J}_T$  is non-singular and the generalized errors  $\boldsymbol{\varepsilon}$  do not depend on the configuration, then  $\boldsymbol{\varepsilon}$  is obtained simply by inverting  $\mathbf{J}_T$ :

$$\boldsymbol{\varepsilon} = \mathbf{J}_T^{-1} \cdot \Delta \mathbf{X}_T \quad (9)$$

If  $\mathbf{J}_T$  is singular then clearly Equation (9) cannot be applied. This can occur if some of the generalized errors,  $\boldsymbol{\varepsilon}_i$ , result in end-effector errors in same direction. By measuring this end-effector error it is not possible to distinguish the amount of the error contributed by each generalized error  $\boldsymbol{\varepsilon}_i$ . This condition usually occurs because of the existence of special geometric conditions between the manipulator joint axes such as parallel or orthogonal axes, or the existence of prismatic joints (Hayati et al., 1988). Partial measurement of vector  $\Delta \mathbf{X}$ , such as measuring only the position but not the orientation of the end-effector, can also lead to a singular  $\mathbf{J}_T$ . In this case only linear combinations of generalized errors  $\boldsymbol{\varepsilon}_i$  can be calculated. Mathematically, the singularity of  $\mathbf{J}_T$  is expressed with a linear dependency of the columns of  $\mathbf{J}_T$ . Equation (9) also cannot be successfully applied when some of the generalized errors depend on the manipulator configuration, namely  $\boldsymbol{\varepsilon}(\mathbf{q})$ . For example, the generalized errors created by deflections depend on the configuration. The procedure to find  $\boldsymbol{\varepsilon}$  for a singular  $\mathbf{J}_T$  or for  $\boldsymbol{\varepsilon} = \boldsymbol{\varepsilon}(\mathbf{q})$  is described below.

## Reduction of $\mathbf{J}_T$ to a Non-Singular Matrix

If the columns of  $\mathbf{J}_T$  are reduced to a linear independent set by grouping the generalized errors that correspond to linear dependent columns then  $\mathbf{J}_T$  can be made non-singular.

If  $\lambda$  is an eigenvalue of  $\mathbf{J}_T$  and  $\mathbf{c}$  the corresponding eigenvector then:

$$\mathbf{J}_T \cdot \mathbf{c} = \lambda \cdot \mathbf{c} \quad (10)$$

If  $\mathbf{J}_T$  is singular, several of its eigenvalues are zero. Let  $\mathbf{c}^i = [c_1^i \ c_2^i \ \dots \ c_r^i]^t$  be the  $i^{\text{th}}$  eigenvector that corresponds to a null eigenvalue where  $r$  is equal to  $6n$  which is the maximum dimension of  $\mathbf{J}_T$  and the superscript "t" denotes the transpose of a vector. Then Equation (10) is written as:

$$\mathbf{J}_T \cdot \mathbf{c}^i = [\mathbf{J}_T^1; \mathbf{J}_T^2; \dots; \mathbf{J}_T^r] \cdot \mathbf{c}^i = \mathbf{J}_T^1 \cdot c_1^i + \mathbf{J}_T^2 \cdot c_2^i + \dots + \mathbf{J}_T^r \cdot c_r^i = 0 \quad (11)$$

From Equation (11) it can be seen that the coordinates of the eigenvector  $\mathbf{c}^i$  are the coefficients of linear dependent columns of  $\mathbf{J}_T$ . Assuming that in total,  $\mathbf{J}_T$  has  $r$  eigenvectors corresponding to a null eigenvalue, these eigenvectors can form a matrix  $\mathbf{C}$ :

$$\mathbf{C} = [\mathbf{c}^1; \mathbf{c}^2; \dots; \mathbf{c}^r] \quad (12)$$

Matrix  $\mathbf{C}$  represents a basis of a linear space composed of vectors that when multiplied with  $\mathbf{J}_T$  result in zero. After performing linear combinations of rows of matrix  $\mathbf{C}$ , it is obtained in a reduced row echelon form (Leon, 1994). In this form matrix  $\mathbf{C}$  is composed of many zero elements, and hence it is very easy to distinguish the linear dependent columns of  $\mathbf{J}_T$ . By inspection of the elements of each column of matrix  $\mathbf{C}$ , the sets of linear dependent columns of  $\mathbf{J}_T$  are identified. From each set, one column is kept in  $\mathbf{J}_T$ , the others are deleted and the generalized errors that correspond to these linear dependent columns form linear combinations using the coefficients of the column of matrix  $\mathbf{C}$ . An example is given next, to illustrate this procedure.

Assume that one column of matrix  $\mathbf{C}$ , after its reduction to row echelon form, has all its elements equal to zero except the elements of the  $i^{\text{th}}$  and  $j^{\text{th}}$  rows, that are equal to 1 and -1 respectively. From Equation (11) it can be deduced that  $i^{\text{th}}$  and  $j^{\text{th}}$  columns of  $\mathbf{J}_T$  are equal:

$$[\mathbf{J}_T^1 \dots \mathbf{J}_T^i \dots \mathbf{J}_T^j \dots \mathbf{J}_T^r] \cdot [0 \dots 1 \dots -1 \dots 0]^t = 0 \Rightarrow \mathbf{J}_T^i = \mathbf{J}_T^j \quad (13)$$

For example, using Equation (8) it can be seen that the generalized errors  $\epsilon_i$  and  $\epsilon_j$  corresponding to  $i^{\text{th}}$  and  $j^{\text{th}}$  columns of  $\mathbf{J}_T$  can be grouped into one new error  $\epsilon_{ij}$  which is their sum, and one of the columns either  $i^{\text{th}}$  or  $j^{\text{th}}$  of  $\mathbf{J}_T$  can be eliminated:

$$\Delta \mathbf{X}_T = \mathbf{J}_T \cdot \mathbf{e} = \mathbf{J}_T^1 \mathbf{e}_1 + \dots + \mathbf{J}_T^i \mathbf{e}_i + \dots + \mathbf{J}_T^j \mathbf{e}_j + \dots + \mathbf{J}_T^r \mathbf{e}_r = \mathbf{J}_T^1 \mathbf{e}_1 + \dots + \mathbf{J}_T^i (\mathbf{e}_i + \mathbf{e}_j) + \dots + \mathbf{J}_T^r \mathbf{e}_r \quad (14)$$

The same procedure can be applied to every column of matrix  $\mathbf{C}$  and thus  $\mathbf{J}_T$  can be reduced to a non-singular matrix  $\mathbf{J}_{er}$  and vector  $\mathbf{e}$  is reduced to vector  $\mathbf{e}_r$  composed of linear combinations of the elements of  $\mathbf{e}$ . Hence, Equation (8) is written as:

$$\Delta \mathbf{X}_T = \mathbf{J}_{er} \cdot \mathbf{e}_r \quad (15)$$

The linear dependencies of columns of  $\mathbf{J}_T$  are the same between the columns of matrix  $\mathbf{J}_e$  used in Equation (6). Therefore Equation (6) can be written as:

$$\Delta \mathbf{X} = \mathbf{J}_{er} \cdot \mathbf{e}_r \quad (16)$$

where  $\mathbf{J}_{er}$  is the reduced error Jacobian matrix of the manipulator, after linear dependent columns have been eliminated. Equation (16) is the new error model of the system and can be used in the error compensation scheme described in Figure 2.

### Polynomial Approximation of the Generalized Errors

In general, the elements of vector  $\mathbf{e}_r$  are not constant but depend on the system configuration, payload weight or other non-geometric parameters such as temperature. An example are the generalized errors due to deflections: they depend on

both the system configuration and payload weight, namely  $\mathbf{e}_r(\mathbf{q}, \mathbf{w})$ . So, vector  $\mathbf{e}_r$  cannot be calculated by inverting Equation (15) because  $\mathbf{e}_r$  is not the same at all different configurations where  $\Delta \mathbf{X}$  is measured. In this case, the  $i^{\text{th}}$  element of vector  $\mathbf{e}_r$  must be defined as a function of  $\mathbf{q}$  and  $\mathbf{w}$ . For simplicity of calculation, these functions are approximated by polynomial series expansions of the form:

$$\epsilon_{r,i} = \sum_j \epsilon_{r,i}^{(j)} \cdot (q_1^{a_1} \cdot q_2^{a_2} \cdot \dots \cdot q_n^{a_n} \cdot w_m^b) \quad (17)$$

where  $q_1, q_2, \dots, q_n$  are the manipulator joint parameters,  $w_m$  is an element of the wrench vector from the end-effector, and  $\epsilon_{r,i}^{(j)}$  are the polynomial coefficients.

Theoretically, there is an infinite number of terms in Equation (17). However, for a desired accuracy of the method, only a few terms are used and their coefficients need to be calculated. From the definition of the generalized errors, the errors associated with the  $i^{\text{th}}$  link depend only on the parameters of the  $i^{\text{th}}$  joint. If elastic deflections of link  $i$  are considered, then the generalized errors created by these deflections would depend on the weight wrench  $w_i$  applied at the  $i^{\text{th}}$  link. For a serial manipulator, this wrench is due to the weight of the payload and to the configuration of the links after the  $i^{\text{th}}$ . Hence, the wrench  $w_i$  depends only on the joint parameters  $q_{i+1}, \dots, q_n$ . Thus, the number of terms in the products of Equation (17) can be reduced.

In Equation (17) the coefficients  $\epsilon_{r,i}^{(j)}$  are constant parameters and become the new unknowns of the problem. Equation (17) is substituted into (15), all coefficients  $\epsilon_{r,i}^{(j)}$  are grouped into one vector,  $\mathbf{e}_E$ , and the part of Equation (17) that is known is incorporated into matrix  $\mathbf{J}_T$  and forms a new matrix  $\mathbf{J}_{TE}$ . Then Equation (15) becomes:

$$\Delta \mathbf{X}_T = \mathbf{J}_{TE} \cdot \mathbf{e}_E \quad (18)$$

Vector  $\mathbf{e}_E$  is calculated by inverting Equation (18). The minimum number of configurations where  $\Delta \mathbf{X}$  is measured depends on the number of terms used in Equation (17) to approximate  $\mathbf{e}_r$ . To increase the accuracy of inversion of matrix  $\mathbf{J}_{TE}$  more measurements then needed are made and a least mean square procedure is used to invert Equation (18):

$$\hat{\mathbf{e}}_E = (\mathbf{J}_{TE}^t \cdot \mathbf{J}_{TE})^{-1} \cdot \mathbf{J}_{TE}^t \cdot \Delta \mathbf{X}_T \quad (19)$$

The method of identifying the generalized errors is summarized in Figure 3.

### APPLICATION TO THE PATIENT POSITIONING SYSTEM

The PPS is a six degree of freedom robot manipulator (see Figure 4) built by General Atomics (General Atomics, 1995; Flanz et al., 1996). The first three joints are prismatic, with maximum travel of 225cm, 56cm and 147cm for the lateral (X), vertical (Y) and longitudinal (Z) axes, respectively. The

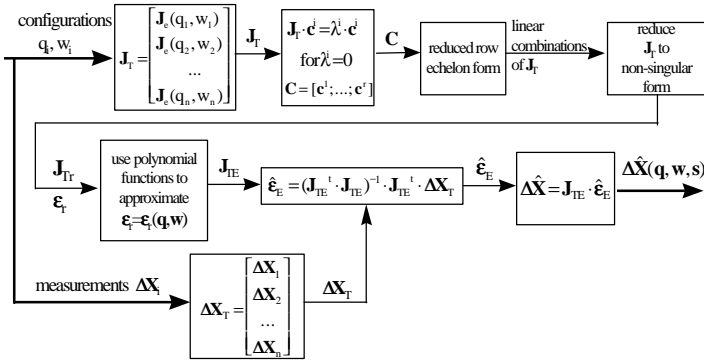


**Figure 3: Flow-chart of the Method to Identify Generalized Errors**

last three joints are revolute joints. The first joint rotates parallel to the vertical (Y) axis and can rotate  $\pm 90^\circ$ . The last two joints are used for small corrections around an axis of rotation parallel to the Z (roll) and X (pitch) axes, and have a maximum rotation angle of  $\pm 3^\circ$ . The manipulator "end-effector" is a couch which supports the patient in a supine position, accommodating patients up to 188 cm in height and 300 lbs in weight in normal operation.

The intersection point of the proton beam with the gantry axis of rotation is called the system isocenter. The couch treatment volume is defined by a treatment area on the couch of 50cm x 50cm and a height of 40cm (see Figure 4). This area covers all possible locations of treatment points (i.e. tumor locations at a patient). The objective is that the PPS makes any point in this volume be coincident with the isocenter at any orientation.

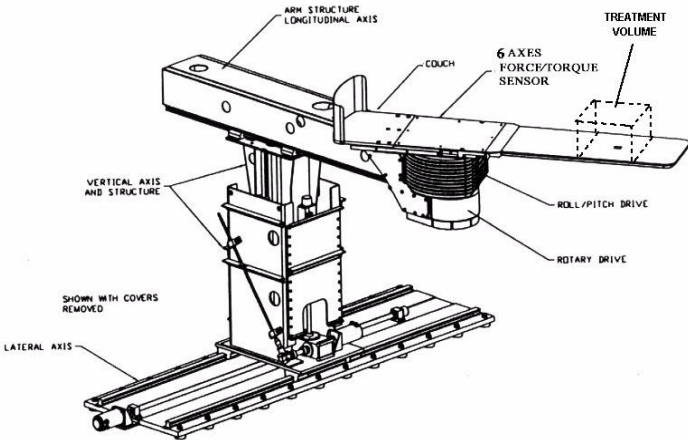


**Figure 4: The Patient Positioning System**

The joint parameters of the PPS are the displacements  $d_1, d_2, d_3$  of the three prismatic joints and the rotations  $\theta, \alpha, \beta$  of the three rotational joints. A 6 axes force/torque sensor is placed between the couch and the last joint. By measuring the forces and moment at this point, it is possible to calculate the patient

weight and the coordinates of the patient center of gravity. The system motions are very slow and smooth due to safety requirements. Hence, the system is quasi-static, and its dynamics do not influence the system accuracy and are neglected.

The accuracy of the PPS was measured using a Leica 3D Laser Tracking System (Leica, 1997). More specifically the measurements were to evaluate the PPS repeatability, the nonlinearity of its weight dependent deflections, the inherent uncompensated PPS accuracy, and the method developed above.

Three targets were placed on the couch at the positions  $P_1, P_2$  and  $P_3$ , shown in Figure 5. The targets are located about 10mm above the couch. The position accuracy of the measurements is approximately 0.04mm.

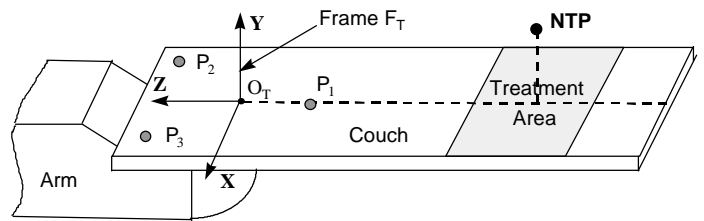


**Figure 5: Close View of the Couch**

A reference frame  $F_T$  is fixed to the couch (see Figure 5). The intersection point of the plane ( $P_1 P_2 P_3$ ) with the Y axis of the fixed reference frame is called  $O_T$ . A fixed reference frame,  $F_o$ , is used to express the coordinates of all points. When the PPS is at its home configuration (all joint variables set equal to zero) the reference frames  $F_T$  and  $F_o$  are coincident.

The location of a tumor on a patient, defined as the Nominal Treatment Point (NTP), is specified in the frame coordinate  $F_T$ . For the results presented below, the NTP coordinates in  $F_T$  are taken as (0, 90, -840) mm.

For more than 700 cases (at different configurations of the PPS and using different weights) the location of points  $P_1, P_2$  and  $P_3$  in frame  $F_o$  was measured and the NTP coordinates in frame  $F_o$  calculated. From the system kinematic model with no errors, the ideal coordinates of NTP were calculated and subtracted from the experimentally measured values to yield the vector  $\Delta X(q, w)$ .

In this work, 450 measurements were used to evaluate the basic accuracy of the PPS, and later used to evaluate the accuracy of the compensation method described above. For this preliminary equation two different payloads were considered: one with no weight and another with a 154 lbs weight at the center of the treatment area. The PPS configurations used were grouped into two sets:

Set a) *Treatment Volume*. The 8 vertices of the treatment volume (see Figure 4) are reached with the NTP with angle  $\theta$

taking values from  $-90^\circ$  to  $90^\circ$  with a step of  $30^\circ$ , for a total of 112 configurations.

Set b) *Independent Motion of Each Axis*. Each axis is moved independently while all other axes are held at the home (zero) values. The step of motion for  $d_1$  is 50 mm, for  $d_2$  20 mm, for  $d_3$  25mm and for  $\theta$   $5^\circ$ , resulting in 338 configurations.

The PPS uncompensated accuracy combining the two sets is shown in Figure 6. The dots represent the positioning errors of NTP. It is clearly seen that inspite of the high quality of the PPS physical system, its uncompensated accuracy is on the order of 10mm. This is approximately 20 times higher than the specification.

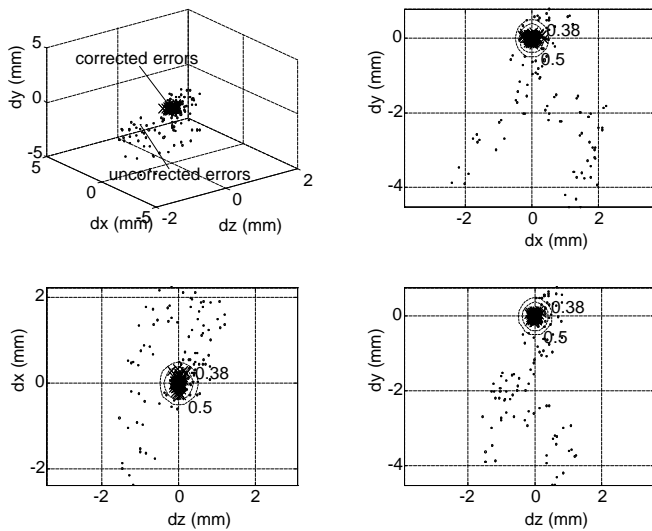


**Figure 6: Measured and Residual Errors After Compensation**

The repeatability error is due to the random system errors, and it cannot be compensated by a model based technique. It represents the accuracy limit of any error compensation algorithm and it also shows how well an error compensation technique performs. Here the repeatability was based on how well the system would return the NTP to certain arbitrary configurations. A total of 270 measurements were taken with zero payload weight. Figure 7 shows the distributions of the repeatability error for each axis. The repeatability error can be seen to be less than 0.15mm ( $3\sigma$ ). Thus this system with a specification of 0.50mm is a good candidate for a model based error correction method.

In implementing the method a general nonlinear function of the wrench  $\mathbf{w}$  can be used. To help establishing this function, the behavior of the PPS positioning errors for different payload weights was examined with measurements made at the home (zero) configuration. The weights ranged from 0 to 300 lbs in steps of approximately 25 lbs. The results showed that the positioning errors of the PPS are nearly linear with the payload weight. The least square error is less than 0.1mm for the linear fit.

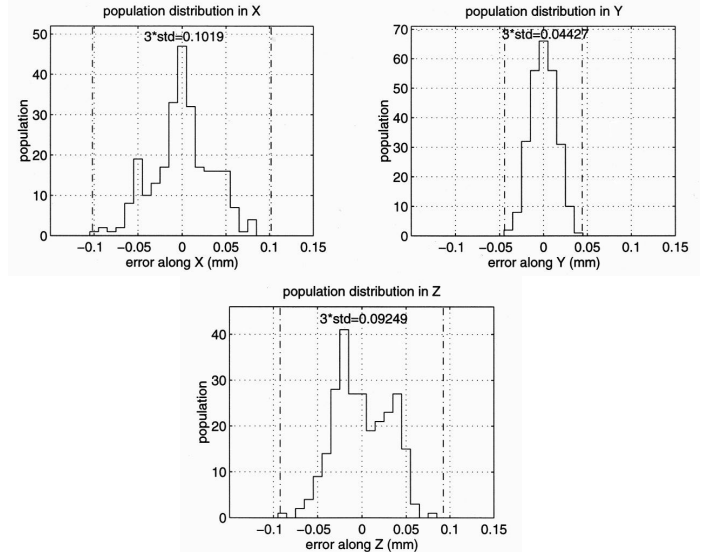


**Figure 7: Repeatability Distribution**

The generalized errors are calculated with Equation (19) using the configurations of set (b) (independent motion of its axes) and half of the treatment volume data (set a). For a Pentium PC 166MHz, the computing time was less than two minutes. The PPS is then commanded to go to compensated points (see Figure 2) for the remaining configurations of set (a). The residual positioning errors of the PPS after compensation for these points are shown in Figure 6. The residual errors are enclosed in a sphere of 0.38mm radius which is smaller than the sphere of 0.5mm radius that represents the accuracy specification. The required number of data points for this calculation was less than 400. The error distribution along each axis is shown in Figure 8. Hence the compensation approach used in this paper enables the system to meet its specification.

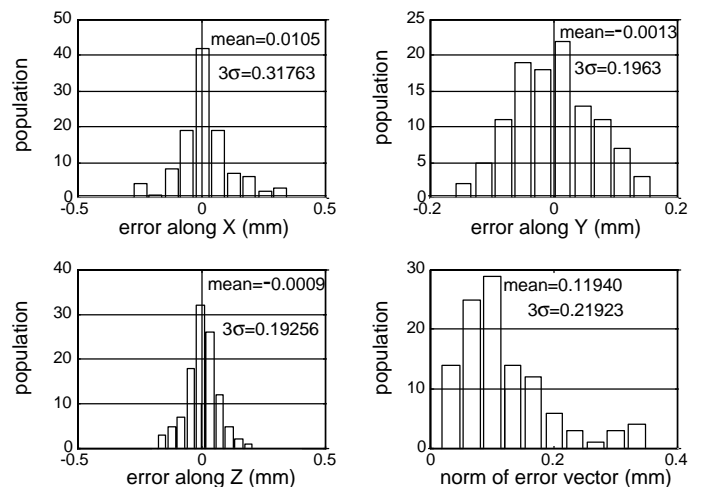


**Figure 8: Statistical Results at NTP**

## CONCLUSIONS

In this paper, a method is presented to identify the positioning end-effector errors of large manipulators. The method can identify the sources of the end-effector errors, both geometric and elastic errors. Previous calibration techniques didn't explicitly consider the wrench at the end-effector to compensate for elastic errors. This method considers the weight dependency without the need to develop an elastic model of the system. It is evaluated experimentally on a high accuracy large medical manipulator. The results showed that the basic accuracy of the manipulator exceeded its specifications, but after applying the method to compensate for end-effector errors the accuracy specifications are met.

## ACKNOWLEDGMENTS

The support of the NIH via the Northeast Proton Therapy Center from the Massachusetts General Hospital for this work and the technical information provided by General Atomics, San Diego, CA are acknowledged.

## REFERENCES

- Borm, J.H. and Menq, C.H., 1991, "Determination of Optimal Measurement Configurations for Robot Calibration Based on Observability Measure", *The International Journal of Robotics Research*, **10**(1): 51-63.
- Broderick, P. and Cirpa, R., 1988, "A Method for Determining and Correcting Robot Position and Orientation Errors Due to Manufacturing", *Transactions of the ASME, Journal of Mechanisms, Transmissions and Automation in Design*, **110**: 3-10.
- Drouet, P., Dubowsky, S. and Mavroidis, C., 1998, "Compensation of Geometric and Elastic Deflection Errors in Large Manipulators Based on Experimental Measurements: Application to a High Accuracy Medical Manipulator", submitted to the *6th International Symposium on Advances in Robot Kinematics*, Austria.
- Dubowsky, S., Maatuk, J. and Perreira, N.D., 1975, "A Parametric Identification Study of Kinematic Errors in Planar Mechanisms". *Transactions of the ASME, Journal of Engineering for Industry*, 635-642.
- Everett, L.J., Lin, C.Y., 1988, "Kinematic Calibration of Manipulators with Closed Loop Actuated Joints", *Proceedings of the 1988 IEEE International Conference of Robotics and Automation*, 792-797.
- Everett, L.J., Lei, J., 1995, "Improved Manipulator Performance Through Local D-H Calibration", *Journal of Robotics Systems*, **12**(7): 505-514.
- Flanz, J. et al., 1995, "Overview of the MGH-Northeast Proton Therapy Center: Plans and Progress", *Nuclear Instruments and Methods in Physics Research B*, **99**: 830-834.
- Flanz, J., et al., 1996, "Design Approach for a Highly Accurate Patient Positioning System for NPTC." *Proceedings of the PTOOG XXV and Hadrontherapy Symposium*, Belgium, September.
- General Atomics, 1995, *Patient Positioner Preliminary Design Documents*.
- Hamel W., Marland S. and Widner T., 1997, "A Model-Based Concept for Telerobotic Control of Decontamination and Dismantlement Tasks," *Proceedings of the 1997 IEEE International Conference of Robotics and Automation*, Albuquerque, New Mexico, April.
- Hayati, S., Tso, K., Roston, G., 1988, "Robot Geometry Calibration", *Proceedings of the 1988 IEEE International Conference of Robotics and Automation*, 947-951.
- Hollerbach, J., 1988, "A Survey of Kinematic Calibration." *Robotics Review*, Khatib O. et al editors, Cambridge, MA; MIT Press.
- Hollerbach, J.M., Wampler, C.W., 1996, "The Calibration Index and Taxonomy for Robot Kinematic Calibration Methods", *International Journal of Robotics Research*, **15**(6): 573-591.
- Leica, 1997, Web Page of Leica Geosystems, <http://www.leica.com/surv-sys/index.asp>.
- Leon, S., 1994, *Linear algebra with applications*. Indianapolis; Macmillian College Publishing Company.
- Mavroidis, C., Dubowsky, S., Drouet, P., Hintersteiner, J., Flanz, J., 1997, "A Systematic Error Analysis of Robotic Manipulators: Application to a High Performance Medical Robot," *Proceedings of the 1997 IEEE International Conference of Robotics and Automation*, Albuquerque, New Mexico, April.
- Mirman, C. and Gupta, K., 1993, "Identification of Position Independent Robot Parameter Errors Using Special Jacobian Matrices". *International Journal of Robotics Research*, **12**(3): 288-298.
- NPTC, 1996, Web Page of the Northeast Proton Therapy Center at the Massachusetts General Hospital, <http://www.mgh.harvard.edu/depts/nptc.htm>.
- Rabinowitz, I. et al, 1985, "Accuracy of Radiation Field Alignment in Clinical Practice." *International Journal of Radiation Oncology, Biology and Physics*, **11**: 1857-1867.
- Roth, Z.S., Mooring, B.W., Ravani, B., 1986, "An Overview of Robot Calibration". *IEEE Southcon Conference*, Orlando, Florida.



Slocum, A., 1992, *Precision Machine Design*. Englewood Cliffs.

Vaichav, R. and Magrab, E., 1987, "A General Procedure to Evaluate Robot Positioning Errors." *The International Journal of Robotics Research*, **6**(1): 59-74.

Vaillancourt C. and Gosselin, G., 1994, "Compensating for the Structural Flexibility of the SSRMS with the SPDM," *Proceedings of the International Advanced Robotics Program, Second Workshop on Robotics in Space*, Canadian Space Agency, Montreal, Canada.

Waldron, K. and Kumar, V., 1979, "Development of a Theory of Errors for Manipulators." *Proceedings of the Fifth World Congress on the Theory of Machines and Mechanisms* : 821-826.

Whitney, D.E., Lozinski, C.A., Rourke, J.M., 1986, "Industrial Robot Forward Calibration Method and Results". *Transactions of the ASME, Journal of Dynamic Systems, Measurement and Control*, 108: 1-8.

Wu, C., 1984, "A Kinematic CAD Tool for the Design and Control of a Robot Manipulator." *The International Journal of Robotics Research*, **3**(1): 58-67.

Zhuang, H., Roth, Z. and Hamano, F., 1992, "A Complete and Parametrically Continuous Kinematic Model for Robot Manipulators". *IEEE Transaction in Robotics and Automation*, **8**(4): 451-462.

Zhuang, H., Roth, Z.S., 1993, "A Linear Solution to the Kinematic Parameter Identification of Robot Manipulators". *IEEE Transactions in Robotics and Automation*, **9**(2): 174-185.

Zhuang, H, Wang, L.K., Roth, Z.S., 1993, "Error-Model-Based Robot Calibration Using a Modified CPC Model". *Robotics and Computer Integrated Manufacturing*, 10(4): 287-299, Great Britain.

Zhuang, H., Wang, K. and Roth, Z., 1994, "Optimal Selection of Measurement Configurations for Robot Calibration Using Simulated Annealing." *Proceedings of the IEEE 1994 International Conference in Robotics and Automation* : 393-398, San Diego, CA.

Zhuang, H., Wu, J., Huang, W., 1996, "Optimal Planning of Robot Calibration Experiments by Genetic Algorithms". *Proceedings of the IEEE 1996 International Conference in Robotics and Automation* : 981-986, Minneapolis, Minnesota.